chemengineering

MDPI

Article

Application of Mathematical Modelling to Reducing and Minimising Energy Requirement for Oxygen Transfer in Batch Stirred Tank Bioreactors

John J. Fitzpatrick *, Franck Gloanec, Elisa Michel, Johanna Blondy and Anais Lauzeral

Process & Chemical Engineering, School of Engineering, University College Cork, Cork T12YT20, Ireland; franck.gloanec@ensiacet.fr (F.G.); elisa_michel@aol.fr (E.M.); johannablondy@gmail.com (J.B.); lauzeral.anais@gmail.com (A.L.)

* Correspondence: j.fitzpatrick@ucc.ie

Received: 27 September 2018; Accepted: 30 January 2019; Published: 3 February 2019

Abstract: In this study, microbial kinetic and oxygen transfer modelling coupled with energy analysis was applied to investigate how manipulation and control of agitator power input and air flowrate can reduce and minimise the total energy requirement in a batch aerobic bioprocess subject to constraints. The study showed that major energy savings can be made by appropriate selection of these variables and how they are controlled throughout a bioprocess. In many bioprocesses, the oxygen concentration in the liquid is controlled at a constant value. This may be achieved by maintaining the agitator power at a constant value and varying the air flowrate or vice versa, or by continuously varying both. The modelling showed that the minimum or near-minimum total energy requirement occurred when operating at the onset of impeller flooding throughout the bioprocess by continuously varying both impeller power and air flowrate over the bioprocess time. Operating at the onset of flooding may not be practical to implement in practice. However, the minimum energy can be approached by dividing the bioprocess time into a small number of time segments with appropriately chosen constant agitator powers and varying the air flowrate within each segment. This is much more practical to implement.

Keywords: energy efficiency; aerobic bioprocess; batch stirred tank bioreactor; mathematical modelling

1. Introduction

In aerobic batch stirred tank bioprocesses, energy is required to transfer sufficient oxygen into the media to satisfy the oxygen requirements of the micro-organisms. Oxygen is supplied to the bioreactor in the form of air that is compressed by a compressor and enters as bubbles from the bottom of the bioreactor. The mechanical agitator improves the oxygen transfer rate through the formation of smaller bubbles and by inducing greater mixing and turbulence that reduces mass transfer boundary layer resistance and disperses the bubbles throughout the vessel. There may be one or more impellers on the agitator shaft depending on the size of the bioreactor. Oxygen supply is critical and can easily become rate-limiting due to its low solubility in water and thus continuous supply is required [1]. Many studies have been conducted to show how agitation and aeration rate influence the oxygen transfer rate and in so doing influence cell growth and metabolite productivity [2–8]. The oxygen requirements of the micro-organisms or oxygen uptake rate (OUR) will vary over the batch bioprocess time because the micro-organisms will grow and increase in number. The aeration system must transfer sufficient oxygen, or the oxygen transfer rate (OTR) must be sufficient to meet the OUR, so that oxygen does not greatly decline and slow the progression of the bioprocess. Oxygen transfer in a bioprocess is strongly influenced by hydrodynamic conditions, which are influenced by operating conditions, the physical-chemical properties of the bioprocess broth, geometrical parameters of the bioreactor

and the oxygen concentration in the broth [1,9–11]. Impeller selection is also very important as the impeller breaks the bubbles into finer bubbles and disperses them throughout the liquid. Flat-blade disc turbines have traditionally been used; however, concave radial turbines can handle higher air flowrates without flooding and their power delivery is less sensitive to air flowrate [12–14].

The main determinants of volumetric mass transfer coefficient (k_La) under direct operational control are agitator mechanical power input per unit volume (Pag/V_L) and the superficial velocity (v_s). Increasing v_s will increase k_La simply because there is more air throughput but this is only up until the impeller starts to flood with air, after which the k_La will decrease. Consequently, the superficial air velocity must be less than the flooding value, which in turn is a function of the agitator Pag/V_L. Measurement and evaluation k_La and how it is influenced by Pag/V_L and v_s is crucial in the design, operation and scale-up of bioprocesses [1,15–20].

The energy or power input associated with the aeration system consists of the following:

- Air compressor power requirement
- Agitator power requirement

Aeration system energy requirement is a significant cost in aerobic bioprocesses [21] and also contributes to the carbon footprint of bioprocesses and associated environmental impact. Reducing aeration system energy and associated costs, as well as the carbon footprint, may be achieved through proper equipment selection, including careful selection of impeller type and impeller diameter to tank ratio [12]. Subsequently, energy minimisation can be achieved by optimal operation of air flowrate and agitator speed [21–24].

Aeration systems may be designed by selecting an air flowrate and sizing an agitator that can meet the maximum OUR requirement without agitator flooding. This results in one air flowrate (and compressor power input) and one agitator power input (referred to as Scenario K in this work) that delivers the required OTR to satisfy the maximum OUR requirement. However, there are potentially many combinations of the two that could deliver this same OTR [23]. These may all have different total energy requirements when the total agitator and compressor energies are summed over the duration of the bioprocess. Consequently, this presents an opportunity to save energy by determining which combination minimises the total energy requirement.

Scenario K is potentially energy inefficient in a batch bioprocess because it uses energy to supply an OTR that satisfies maximum OUR over the entire bioprocess time, whereas the OUR will vary over time, typically being low at the beginning and gradually increasing to a maximum some time during the bioprocess. Thus, this provides an opportunity for energy saving by continuously manipulating the agitator power input and/or air flowrate throughout the whole of the bioprocess time to provide an OTR that matches the OUR throughout the bioprocess [22,23,25].

A commonly used practical control strategy is to maintain the oxygen concentration in the broth at a constant value (referred to as Scenario C in this work) by varying the air flowrate and/or agitator power input throughout the bioprocess. At each time during the bioprocess, there are potentially many combinations of the two that could deliver the same OTR that satisfies the OUR to maintain the oxygen concentration constant [23]. These may all have different total energy requirements when the total agitator and compressor energies are summed over the duration of the bioprocess. Consequently, this presents another opportunity to save energy by manipulating and controlling the agitator power input and/or air flowrate throughout the bioprocess to provide an OTR that matches the OUR in a more energy efficient way [22,23,25].

Even though there has been much work presented in the literature on oxygen transfer there has not been much presented on applying mathematical modelling to energy analysis of oxygen transfer in bioprocesses. Alves and Vasconcelos [21] have performed a mathematical optimisation procedure to minimise total power requirement subject to maintaining the oxygen concentration in the broth at a critical value. The optimisation procedure was applied to a *Streptomyces aureofaciens* bioprocess at its maximum OUR, at both pilot and production scales. The power requirement was compared to

the factory procedure, which set a constant agitator tip speed and evaluated the required air flowrate. The study showed power savings of 10–20% could be achieved by applying the optimisation procedure. Kreyenschulte et al. [26] have developed a computation tool to assess the energy demand at the large scale based on small-scale data. They examined the impact of a number of constraints and showed that the minimum energy consumption for oxygen transfer was achieved by operating close to the onset of flooding for bioreactor volumes of 20 m^3 and larger using conventional agitators.

The objective of this work is to apply microbial kinetic and oxygen transfer modelling coupled with energy analysis to investigate how manipulation and control of agitator power input and air flowrate can reduce and minimise the total energy requirement in an aerobic bioprocess subject to constraints such as impeller flooding. This work contributes to the literature in applying mathematical modelling to practical scenarios (Scenarios K and C) to gain greater insights into how to manipulate the agitator power and air flowrate so as to reduce and minimise the energy requirement in aerobic bioreactors.

2. Mathematical Modelling

The bioreactor considered in this study had a working volume of 20 m^3. A six bladed Rushton turbine impeller was used with a standard design configuration. The height to tank diameter ratio was 1. The tank diameter and cross-sectional area were 2.94 m and 6.8 m^2, respectively. The impeller to tank diameter ratio was 0.35, giving an impeller diameter of 1.03 m.

2.1. Bioprocess Kinetics and Oxygen Uptake

Cell growth is modelled using a first order kinetic model in Equation (1).

$$\frac{dX}{dt} = \mu X \tag{1}$$

where X is cell concentration at time t and μ is the specific growth rate, which is modelled using a Monod type model (Equation (2)):

$$\mu = \frac{\mu_{max} S}{K_S + S}\left(\frac{C_{OL}}{K_O + C_{OL}}\right) \tag{2}$$

where S and C_{OL} are the sugar and oxygen concentrations in the liquid, respectively, and μ_{max}, K_S and K_O are constants.

The product concentration (P) and sugar substrate concentration were modelled using Equations (3) and (4).

$$\frac{dP}{dt} = \alpha\frac{dX}{dt} + \beta X \tag{3}$$

$$\frac{dS}{dt} = -\left(\frac{1}{Y_{XS}}\frac{dX}{dt} + \frac{1}{Y_{PS}}\frac{dP}{dt} + m_S X\right) \tag{4}$$

Suitable values for the constants in the bioprocess model equations are presented in Table 1; these were selected after considering published works in the literature. Values for μ_{max} and K_S can vary significantly and some reported values for μ_{max} varied from 0.09–4.2 h^{-1} [27–30]. K_S values are typically in the mg·L^{-1} range, with reported values typically varying from 0.07 to 200 mg·L^{-1} [27,31,32], although Znad et al. [28] reported a value of 130,900 mg·L^{-1}. K_O can have significant variation but typically it is in the range of 0.1 to 1 mg·L^{-1} [28,32,33]. The values of Y_{XS}, Y_{PS} and m_S were obtained from van't Riet and Tramper [27]. The values of α and β were obtained from Znad et al. [28]. Concentration values at the start of the bioprocess were X_0 = 0.1 g·L^{-1}, S_0 = 150 g·L^{-1} and P_0 = 0 g·L^{-1}, and the bioprocess was completed when S was reduced to 0.1 g·L^{-1}.

Table 1. Values for constants in the bioprocess kinetic model.

μ_{max} (h^{-1})	K_S ($g{\cdot}L^{-1}$)	K_O ($g{\cdot}L^{-1}$)	α	β (h^{-1})	Y_{XS}	Y_{PS}	m_S (h^{-1})
0.25	0.005	0.000363	2.9220	0.1314	0.55	1	0.025

The oxygen uptake rate (OUR) was modelled using Equation (5).

$$OUR = \delta \frac{dX}{dt} + \phi X \tag{5}$$

where δ is the yield of oxygen consumed for cell growth and ϕ is the oxygen consumption coefficient for maintenance.

The values of δ and Φ can vary significantly depending on the bioprocess. The values δ = 0.64 and Φ = 0.032 h^{-1} were selected based on a range of values provided in an OUR review article by Garcia-Ochoa et al. [34].

2.2. Oxygen Transfer and Agitator Mechanical Power

The mass transfer Equation (6) was used to model the oxygen transfer rate:

$$OTR = K_L a(C^*_{OL} - C_{OL}) \tag{6}$$

where

$$C^*_{OL} = \frac{C_{OG}}{M} \tag{7}$$

C_{OG} is the oxygen concentration in the air bubbles and M is the Henry's law equilibrium constant (= 35). C_{OG} varies from the concentration of oxygen in ambient air (C_{OGI} = 280 $mg{\cdot}L^{-1}$) to the concentration of oxygen in air leaving the bioreactor (C_{OGO}). Thus Equation (8) was used to evaluate an average equilibrium concentration of oxygen in the liquid.

$$C^*_{OL} = \frac{(C_{OGI} + C_{OGO})/2}{M} \tag{8}$$

A mass balance on the bioreactor was used to evaluate another expression for OTR (Equation (9)).

$$OTR = \frac{F_G}{V_L}(C_{OGI} - C_{OGO}) \tag{9}$$

where F_G is the air volumetric flowrate and V_L is the working volume of the bioreactor.

The correlation relationship between $k_L a$, agitator mechanical power input (Pag) and air superficial velocity (v_s) is given by Equation (10).

$$k_L a = K\left(\frac{Pag}{V_L}\right)^{n1}(v_s)^{n2} \tag{10}$$

The values of the constants were K = 0.026, n_1 = 0.4 and n_2 = 0.5, and these were obtained from van't Riet [35]. For a particular bioprocess, the values for these constants need to be determined, as these will be influenced by the physicochemical properties of the bioprocess broth, including its viscosity.

The air superficial velocity is defined in Equation (11).

$$v_s = \frac{F_G}{A_T} \tag{11}$$

where A_T is the cross-sectional area of the bioreactor.

The parameter *vvm* is used in the modelling scenarios because in the bioprocess industry the air flowrate is commonly expressed in terms of *vvm* [12], which is the volume of air per volume of liquid per minute and may be defined by Equation (12).

$$vvm = \frac{F_G}{V_L} \tag{12}$$

where units are expressed in minutes^{-1}.

2.3. Flooding and Phase Equilibrium Constraints

The air flowrate is limited by impeller flooding and this depends on the mechanical power input (*Pag*). The air flowrate (F_{GF}) at the onset of flooding, for a fixed value of *Pag*, was evaluated by solving Equations (13) to (15). Equation (13) was obtained from Bakker et al. [14].

$$N_A = 30(N_{Fr})\left(\frac{D}{T}\right)^{3.5} \tag{13}$$

where

$$N_A = \left(\frac{F_{GF}}{ND^3}\right) \quad and \quad N_{Fr} = \left(\frac{N^2D}{g}\right)$$

D and T are impeller and tank diameters, respectively. Equation (14) is the power number equation.

$$Pag = N_{PG}\rho N^3 D^5 \tag{14}$$

where the density (ρ) = 1 kg·L^{-1}, N is the impeller rotational speed and N_{PG} is the impeller power number. N_{PG} varies with the air flowrate, and Equation (15) was applied to take this into account. This equation was obtained from Bakker et al. [14] along with values for the constants.

$$\frac{N_{PG}}{N_P} = 1 - (b - a\mu)N_{Fr}^{d} \tan h(cN_A) \tag{15}$$

where N_P is the ungassed power number (= 6), μ is the liquid viscosity (5 mPa·s), a = 0.72, b = 0.72, c = 24 and d = 0.25 (flat-bladed turbine impeller).

The oxygen concentration in the air leaving the bioreactor (C_{OGO}) was limited by the phase equilibrium constraint in Equation (16).

$$C_{OGO} \geq M(C_{OL}) \tag{16}$$

2.4. Aeration System Energy Requirement

In the simulations the agitator mechanical power input requirement was either given a value or was estimated using the previous equations, including Equation (10). The compressor mechanical power requirement for a specific air flowrate was estimated from Equation (17) [21].

$$P_C = \frac{\gamma}{\gamma - 1}F_G P_{atm}\left(\left(\frac{P_i}{P_{atm}}\right)^{\frac{\gamma-1}{\gamma}} - 1\right)\left(\frac{1}{\eta_C}\right) \tag{17}$$

where P_{atm} is atmospheric pressure and Pi is the atmospheric pressure plus the static pressure acting on the bottom of the bioreactor due to the weight of liquid, γ = 1.4. η_c is the isentropic efficiency of the compressor (assumed to be constant at 0.7). The sum of the agitator and compressor electrical energy requirements (E_{tot}) for the duration time of the bioprocess (t_f) is given by Equation (18).

$$E_{tot} = \int_0^{t_f} \left(\frac{Pag + P_C}{\eta_m} \right) dt \quad (18)$$

where η_m is the electric motor efficiency (assumed to be constant at 0.9 for both the agitator and compressor).

2.5. Modelling Scenarios

The following scenarios were investigated:

- **Scenario K**: Both *Pag* and *vvm* are maintained as constant. This may occur in some bioprocesses which are operated under fixed conditions of agitator power input and air flowrate.
- **Scenario C**: The oxygen concentration in the liquid is kept constant throughout the bioprocess. This represents a practical control strategy by monitoring oxygen concentration in the liquid and controlling either agitator power input or air flowrate or both to maintain the oxygen concentration at a constant value. This was implemented for the following sub-scenarios:
- **Scenario C1**: *Pag* is kept constant throughout the bioprocess and *vvm* is varied. From an oxygen transfer energy perspective, it is later shown that dividing the bioprocess time up into two or more time segments with different constant *Pag* values and varying *vvm* in each time segment significant energy savings may be obtained (this is referred to as **Scenario C1-N**, where N is the number of time segments).
- **Scenario C2**: *vvm* is kept constant and *Pag* is varied.
- **Scenario C3 and Cmin**: Scenario C3 is where both *Pag* and *vvm* are varied. It will be shown later that a *Pag*-*vvm* combination profile over time can be evaluated that minimises the total electrical energy required for a specified constant oxygen concentration in the liquid. This is referred to as scenario *Cmin*.

These scenarios were modelled to investigate where the minimum total energy requirement existed within each scenario and to elucidate the rationale, and to compare the energy requirements obtained for the different scenarios. This information was then used to highlight how air flowrate and agitator power input can be manipulated to reduce and minimise the total energy requirement. These scenarios were subjected to a number of constraints including impeller flooding, phase equilibrium and oxygen starvation. There are other possible constraints such as foaming, carbon dioxide inhibition, maximum impeller rotational speed, minimum agitator speed for acceptable mixing and minimum allowable heat transfer coefficient [21,26], but these were not considered in this work.

2.6. Model Implementation

A numerical method approach was used to carry out the computations where algorithms using the equations above were developed for each scenario. The computations were implemented in Matlab. In Scenario K, where the oxygen concentration in the liquid varied over time, the following mass balance was used to evaluate the oxygen concentration at the end of each time step (C_{OLf}):

$$C_{OLf} = (OTR - OUR)\Delta t + C_{OLi} \quad (19)$$

where Δt is the time duration of the time step and C_{OLi} is the oxygen concentration at the beginning of the time step.

3. Results and Discussion

3.1. Bioprocess Progression

The evolution of the sugar, product and cell concentrations are presented in Figure 1a for a simulation where the specific growth rate is near to its maximum of 0.25 h^{-1} for much of the bioprocess time. The bioprocess progresses slowly up to about 10 hours, after which there are significant changes

in concentrations; the bioprocess ends at about 24 hours. The evolution of OUR is also presented in Figure 1a, where the OUR reaches a maximum of 4.7 $g \cdot L^{-1} \cdot h^{-1}$ towards the end of the bioprocess. Figure 1b shows the influence of oxygen and sugar concentrations in the bioprocess liquid on the specific growth rate. The oxygen concentration has a major impact on specific growth rate. The specific growth rate is near to its maximum at the high oxygen concentration of 8 $mg \cdot L^{-1}$. It slowly decreases as the oxygen concentration is reduced to about 2 $mg \cdot L^{-1}$, after which there is a more precipitous decrease (it may be noted that K_O is 0.363 $mg \cdot L^{-1}$). On the other hand, the sugar concentration during the bioprocess varies from 150 $g \cdot L^{-1}$ down to 0.1 $g \cdot L^{-1}$ and this does not have a major influence on specific growth rate, as illustrated in Figure 1b.

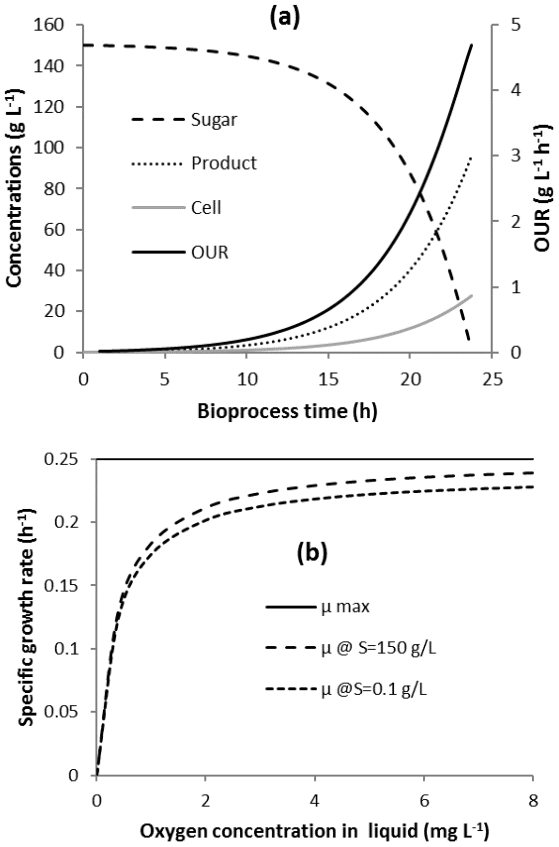

Figure 1. Microbial kinetics: (**a**) cell, sugar and product concentrations and oxygen uptake rate (OUR) (Scenario K: *Pag* = 45 kW; *vvm* = 1); (**b**) effect of oxygen and sugar concentrations on specific growth rate.

3.2. Scenario K

In this scenario both *Pag* and *vvm* are kept constant during each bioprocess run. There are constraints that place restrictions of feasible combinations of *vvm* and *Pag* values that allow the bioprocess to achieve completion. Impeller flooding places an upper limit on *vvm* for a given *Pag*, and Equations (13) to (15) were used to estimate the flooding *vvm* for each *Pag*. As *vvm* decreases, the oxygen concentration in the bioprocess liquid will also decrease, leading to longer bioprocess times. The microbes may suffer from "oxygen starvation" and die at low oxygen concentrations; a lower limit of oxygen concentration was thus applied as a constraint in the model. This was given a low value of 0.01 $mg \cdot L^{-1}$. This constraint on oxygen concentration places a lower value constraint on *vvm* for a given *Pag*. The flooding and oxygen starvation constraints are presented in Figure 2. The region between the flooding curve and the oxygen starvation curve represents feasible combinations of *vvm* and *Pag* that will allow the bioprocess to achieve completion. From Figure 2, the minimum feasible *Pag* is around 15 kW.

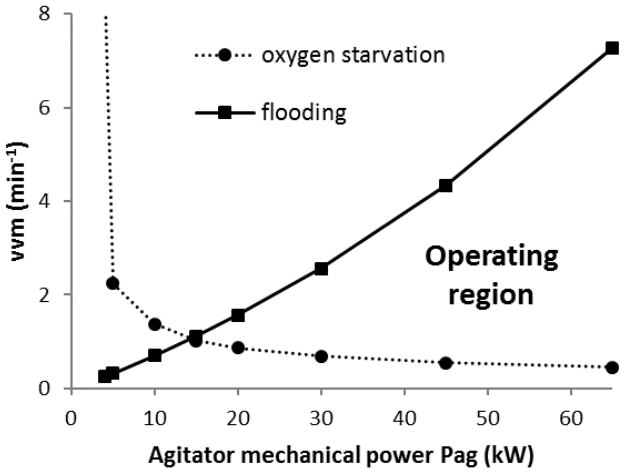

Figure 2. Scenario K: Limiting constraints on *vvm* and agitator mechanical power: oxygen starvation and impeller flooding.

Considering the above, model simulations were run for *Pag* values ranging from 15 kW up to 100 kW, and for *vvm* values ranging in between the oxygen starvation and flooding constraints for each *Pag* value. Looking at one of the *Pag* values in more detail, *Pag* = 45 kW, the influence of *vvm* on the agitator, compressor and total electrical energies, and bioprocess time, is presented in Figure 3. Data is presented for *vvm* values between 0.55, which is close to where oxygen starvation occurs, and 4.3, which is close to where flooding occurs. There is a trade-off between lower *vvm*, leading to lower compressor power, and higher bioprocess time, which increases agitator energy and possibly compressor energy also. This leads to a minimum in total electrical energy of 3.2 GJ; however, this minimum occurs close to the oxygen starvation constraint at *vvm* = 0.55. Figure 4 shows the progression of the oxygen concentration in the bioprocess liquid over time for *Pag* = 45 kW at three values of *vvm* ranging from values close to oxygen starvation (*vvm* = 0.55) to those near to flooding (*vvm* = 4.3). For all three conditions, the oxygen concentration in the liquid is high, beig 7–8 mg L^{-1} over the first 10 hours, which is expected as the OUR is low over this time period. For the lower *vvm* values, C_{OL} decreases more rapidly to lower levels, which results in longer bioprocess times.

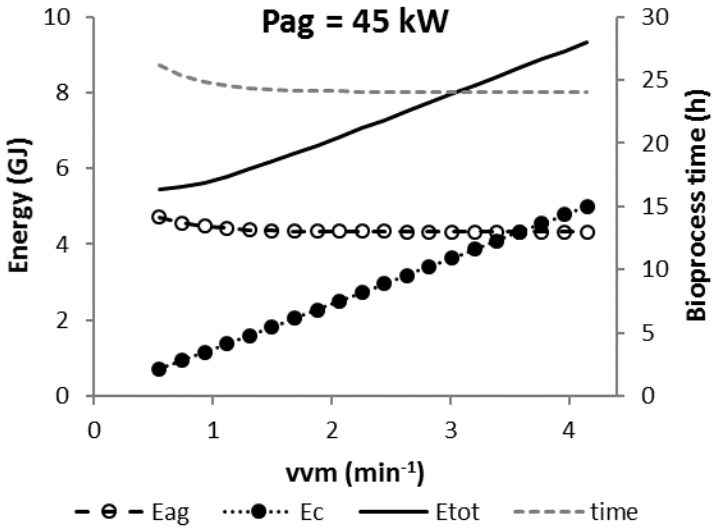

Figure 3. Scenario K: Influence of *vvm* on agitator (*Eag*), compressor (*Ec*) and total (*Etot*) electric energies and bioprocess time for *Pag* = 45 kW.

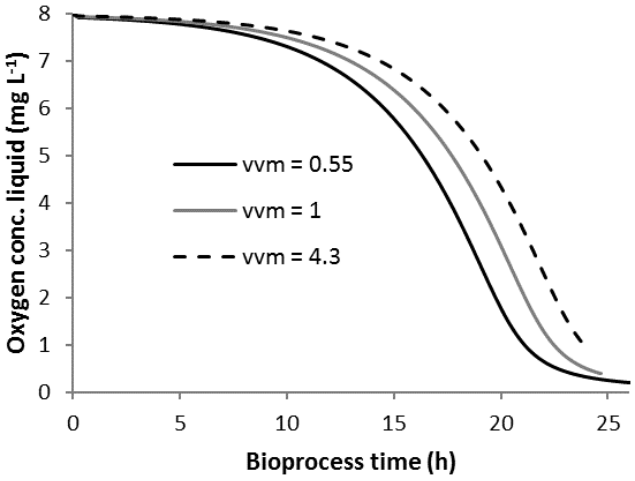

Figure 4. Scenario K: Evolution of oxygen concentration in bioprocess liquid when operating at *Pag* = 45 kW at *vvm* = 0.55, 1 and 4.3.

Figure 5a shows how *Pag* and *vvm* influence the total electric energy requirement. Results are provided for four constant values of *Pag* ranging from 15 to 65 kW. It shows that there are large variations in total energy requirement depending on the values of *Pag* and *vvm* selected and thus there is potential for major energy savings if appropriate values were chosen. Figure 5a shows that lower total energy is required as *Pag* is reduced towards 15 kW. However, the *vvm* operating window is also greatly reduced due to the constraints illustrated in Figure 2.

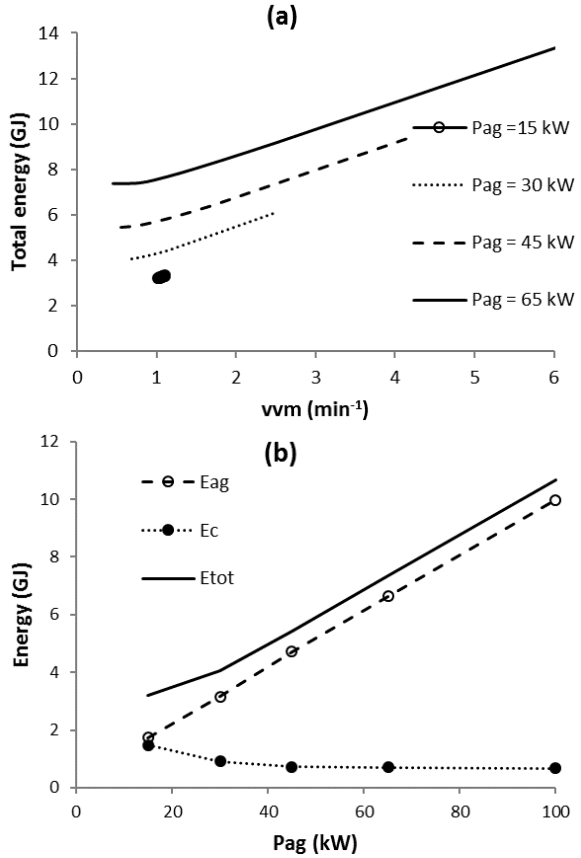

Figure 5. Scenario K: (**a**) Influence of *vvm* on total electric power for constant values of *Pag;* (**b**) Influence of *Pag* on minimum total electric energy requirement (*Etot*) and corresponding agitator (*Eag*) and compressor (*Ec*) electric energy inputs.

Figure 5b shows the minimum total energy requirement at each *Pag* value between 15 and 100 kW, along with the corresponding agitator and compressor energies. The minimum of the total energy minima occurs at the lower extreme of *Pag* = 15 kW. However, this is located at a very sensitive point at the intersection between the flooding and starvation constraints and thus is not to be recommended as a practical operating condition. Figure 5 highlights the large variation in minimum total energy values depending on the selection of *Pag*. It is 4.1 GJ at *Pag* = 30 kW, while it is over 2.5 times greater at 10.7 GJ for *Pag* = 100 kW. This is a large difference depending on the selection of *Pag*. Consequently, there are energy savings to be made from appropriate selection of *Pag*.

3.3. Scenario C

In this scenario C_{OL} is maintained at a constant value throughout the bioprocess. This may be achieved by keeping *vvm* constant and varying *Pag*, or by keeping *Pag* constant and varying *vvm*, or by varying both *Pag* and *vvm*. This results in a number of corresponding sub-scenarios which are investigated in the following sections. Firstly, the constant values of C_{OL} to be investigated must be stated, and this is highly influenced by the impact of C_{OL} on bioprocess kinetics. C_{OL} can vary between 0 and 8 mg·L^{-1} and Figure 1b shows the impact of C_{OL} on specific growth rate. Considering this, the following constant values of C_{OL} were investigated: 5, 3, 2, 1, 0.4 and 0.1 mg·L^{-1}.

3.4. Scenario C1

In this scenario C_{OL} is maintained constant by varying *vvm* for a constant value of *Pag* throughout the bioprocess. Once *Pag* is fixed, the flooding velocity is also fixed. Below a certain critical value of *Pag*, the *vvm* required at maximum OUR would exceed the flooding velocity and C_{OL} could not be maintained constant. At and above this critical value of *Pag*, *vvm* could be varied to maintain a constant C_{OL} throughout the bioprocess. Consequently, the bioprocess needs to be operated at a *Pag* value equal to or above the critical *Pag* in order to maintain constant C_{OL} throughout the bioprocess. At higher values of *Pag* above the critical value, the *vvm* required would decrease as expected. Furthermore, in the earlier part of the bioprocess when OUR is low, the *vvm* values required were low enough to break the constraint in Equation (16), giving rise to *Cogo* being less than $M \times C_{OL}$. This constraint cannot be broken and it thus limits the OTR that can be provided in Equation (9). To rectify this, *vvm* was increased so that $Cogo = M \times C_{OL}$.

For each constant value of C_{OL}, the agitator, compressor and total energies were evaluated for agitator power values at and above the critical *Pag* value. Figure 6 presents total energy data as a function of constant *Pag* for three different values of C_{OL}. It shows that the constant value of *Pag* chosen has a major impact on total energy requirement and thus care needs to be taken in choosing this value. For a fixed C_{OL}, the minimum total energy occurs at the critical *Pag*, which is the value of *Pag* where flooding will start to occur at the time when OUR is a maximum. This is referred to as C1min. Considering this, it may be more prudent to operate at *Pag* values above the critical *Pag* due to uncertainties associated with flooding correlations.

Figure 6 also shows that the critical *Pag* decreases as C_{OL} decreases. Less *vvm* is required at lower C_{OL} values because the maximum OUR is less and the mass transfer driver is greater, meaning the critical *Pag* is lower. Figure 7 presents the minimum total energy at discrete values of C_{OL} between 0.1 and 5 mg·L^{-1}. The lowest minimum total energy was about 3.8 GJ, which occurred at 0.1 mg·L^{-1} and after a greatly increased bioprocess time of 98 hours. Thus, there is a trade-off between lower minimum total energy values and higher bioprocess times as C_{OL} is reduced.

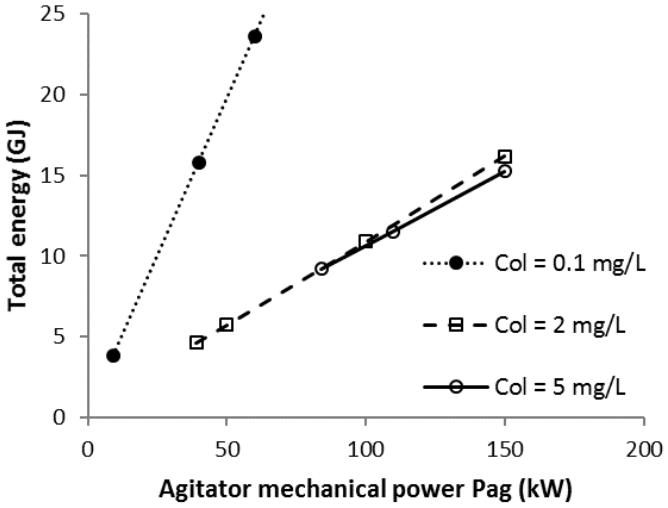

Figure 6. Scenario C1: Influence of constant values of *Pag* and oxygen concentration in the bioprocess liquid (C_{OL}) on total electric energy requirement.

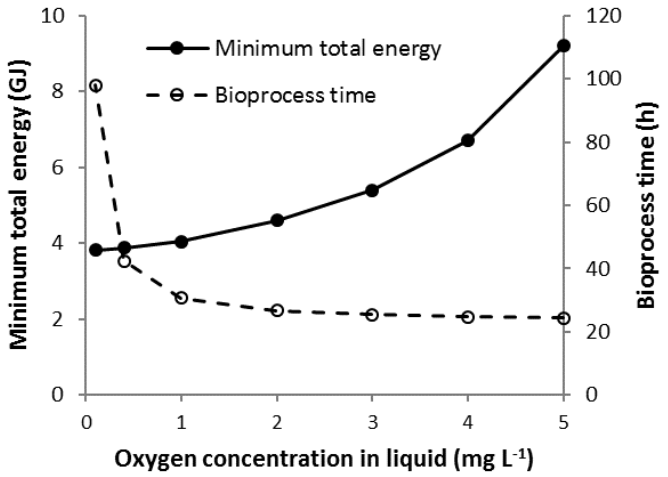

Figure 7. Scenario C1: Influence of oxygen concentration in the liquid on minimum total electric energy requirement.

3.5. Scenario C2

In this scenario C_{OL} is maintained constant by varying *Pag* for a constant value of *vvm* throughout the bioprocess. There exists a minimum *vvm* that must be supplied to meet the maximum OUR and not break the constraint given in Equation (16), i.e., $C_{OGO} \geq M(C_{OL})$. The maximum OUR was evaluated previously and the minimum v_S (v_{S_min}) was estimated, using Equations (9), (11) and (16), to formulate Equation (20), noting that OTR equals OUR when C_{OL} is constant. This was then used to evaluate the minimum *vvm*.

$$v_{S\_min} = \frac{V_L OUR_{max}}{A_T(C_{OGI} - MC_{OL})} \tag{20}$$

Maintaining C_{OL} at a constant value in this scenario was shown to be impossible and thus this scenario was not investigated further. At *vvm* values higher than the minimum, it was found that the *Pag* required, for much of the bioprocess, was so low that the flooding *vvm* was less than *vvm*, meaning the impeller was flooding. To overcome this flooding problem, the *Pag* had to be increased to the onset of the flooding value, which increased OTR and caused C_{OL} to deviate from its constant value for much of the bioprocess.

3.6. Scenario C3

In this scenario C_{OL} is maintained constant by varying both *vvm* and *Pag* throughout the bioprocess. At a specific time during the bioprocess, many different combinations of *vvm* and *Pag* can be evaluated to provide an OTR that satisfies the OUR at that time in order to maintain C_{OL} at a constant value [22,23]. However, the values of *vvm* and *Pag* are subject to the constraints of phase equilibrium and agitator flooding outlined in Section 2.3. A typical evolution of OUR over the bioprocess time is given in Figure 1a. For a constant C_{OL} of 2 mg·L^{-1}, the OUR varies from around 0 up to 4.55 g·L^{-1}·h^{-1}. Simulations were performed to evaluate the effect of *vvm* on the power requirement of the compressor and agitator that could supply the OTR required to satisfy the OUR in the range of 0 up to 4.55 g·L^{-1}·h^{-1}. Figure 8 presents data for an OUR value of 4.5 g·L^{-1}·h^{-1}. As expected, compressor power increases as *vvm* increases and there is a corresponding decrease in agitator power to supply the OTR required to meet the OUR. However, compressor power increases linearly with *vvm* while agitator power decreases in an exponential fashion. The trade-off between compressor and agitator power results in a value of *vvm* that minimises total power. In the simulations for OUR values in the range of 0 up to 4.55 g·L^{-1}·h^{-1}, this minimum tended to be located at a value of *vvm* that was beyond the flooding value. Consequently, the minimum total power that also satisfies the constraints was located at the onset of flooding. Figure 8 also highlights that care needs to be taken in the selection of *vvm*, so as to remain within constraints, especially the flooding constraint, and to avoid excessive total power requirement at lower *vvm*, due to excessive agitator power. Consequently, major savings in aeration system energy requirement can be made by careful selection of *vvm* and agitator power input requirement throughout the bioprocess, and mathematical modelling can assist in this selection.

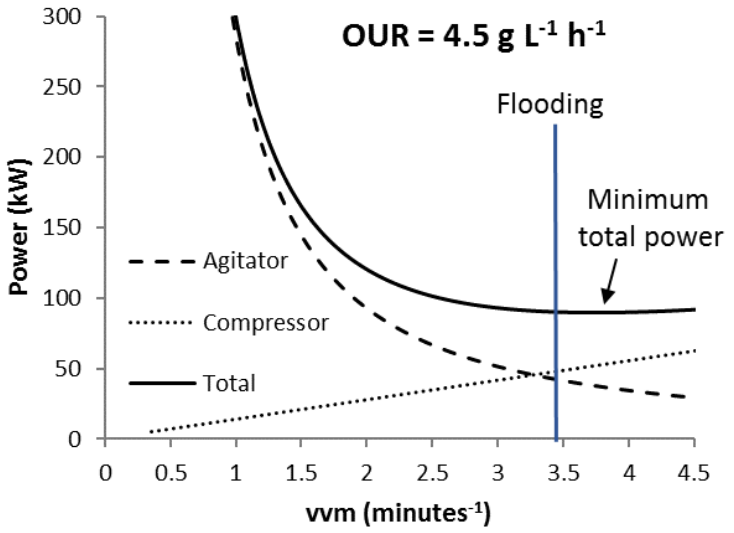

Figure 8. Scenario C3: Influence of *vvm* on compressor, agitator and total electrical power requirements for OUR = 4.5 g·L^{-1}·h^{-1} (C_{OL} = 2 mg·L^{-1}).

3.7. Scenario Cmin

From the above scenario C3 analysis, it may be observed there are specific values of *vvm* (and corresponding air compressor power) and agitator power that minimise the total electrical power requirement to supply the OTR for an OUR at a given time during the bioprocess. This analysis can then be applied over the whole time duration of the bioprocess to evaluate the combinations of *vvm* and *Pag* that minimise the total electrical power requirement at each time increment throughout the bioprocess. This results in the minimum total energy requirement for Scenario C (C_{OL} = constant), which is referred to as Scenario *Cmin*. This analysis was applied to a bioprocess where C_{OL} was kept constant at 2 mg·L^{-1}. Figure 9 shows the variation in *vvm*, compressor power, agitator power and total power over the course of the bioprocess. The values of *vvm* and *Pag* that minimised total power

were at the onset of flooding throughout all of the bioprocess. The oxygen concentration in the air leaving the bioreactor (C_{OGO}) was consistently high throughout the bioprocess, ranging from about 225 to 250 mg·L^{-1}, which is not too far below the inlet oxygen concentration of 280 mg·L^{-1}.

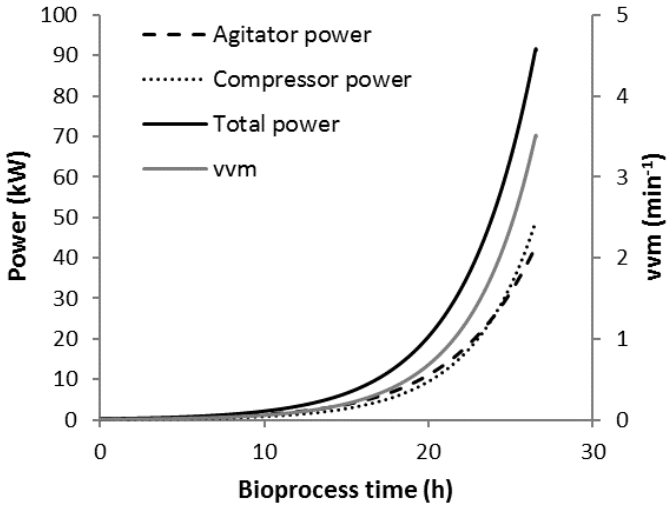

Figure 9. Scenario Cmin: Evolution of *vvm* and compressor, agitator and total electrical power inputs (C_{OL} = 2 mg·L^{-1}).

The power requirements will depend on the values of OUR, working volume, the k_La correlation and the constraints (in particular the flooding constraint). Less vigorous aerobic bioprocesses have maximum OUR values of about 1 g·L^{-1}·h^{-1} while vigorous aerobic bioprocesses have OUR values of around 7 g·L^{-1}·h^{-1} [26]. Kreyenschulte et al. [26] have shown that the minimum total power requirement also occurs at the onset of flooding, but only for bioreactor sizes of around 20 m^3 and larger (the flooding constraint is irrelevant for smaller bioreactors using conventional agitators). Consequently, simulations were also performed at 2.5 m^3 and 100 m^3 for OUR values in the range of 1–7 g·L^{-1}·h^{-1} for the k_La correlation constants used in the current study. The results are presented in the first line of Table 3 and show that the minimum total power requirement was constrained by the onset of flooding for eight of the nine simulations presented. For the other simulation, the total power requirement at flooding was about 0.5% greater than the minimum. These results suggest that the minimum (or near minimum) total energy requirement during a bioprocess can be obtained by operating at the onset of flooding.

The results shown above were obtained using the k_La correlation constants used in the current study (correlation 1 in Table 2). Consequently, further simulations were performed using four other k_La correlations presented in Table 2 and obtained from Benz [20], van't Riet [35] and Bakker [14]. This was to further evaluate if the minimum (or near minimum) total power occurred at the onset of flooding. The results showed that three of the other correlations behaved similarly to the first correlation (Table 3), with minimum total power being constrained by flooding or having a value within 0.5% of that at flooding. However, for correlation 2 (Table 3), the minimum total power occurred before flooding for all the simulations. The total power at onset of flooding was about 1–25% greater than the minimum total power value, with higher values occurring at the smaller volume and bigger OUR values, which is consistent with the work of Keyenschulte et al. [26]. Overall, the data presented for minimising total energy in Scenario C suggest that the *vvm-Pag* combinations should be controlled so that they are at or are close to the onset of flooding to supply an OTR that equals the OUR throughout the bioprocess, although this does depend on the k_La correlation constants and the factors that influence the onset of flooding.

Table 2. Values of constants in k_La correlations.

k_La Correlations and References	Constants		
	K	***n*1**	***n*2**
1—van't Riet non-coalesce [van't Riet, 1979]	0.026	0.4	0.5
2—van't Riet coalesce [van't Riet, 1979]	0.002	0.7	0.2
3—Benz broth 1 [Benz, 2013]	0.015	0.55	0.6
4—Benz broth 2 [Benz, 2013]	0.088	0.542	0.741
5—Bakker [Bakker, 1994]	0.015	0.6	0.6

Table 3. Influence of k_La correlation (Table 2), working volume (V_L) and OUR on whether or not minimum total power occurs at the onset of flooding in Scenario *Cmin*—Y: yes, minimum total power occurs at onset of flooding; N: no, it does not (C_{OL} = 2 mg·L^{-1}).

k_La Correlation	V_L = 2.5 m^3			V_L = 20 m^3			V_L = 100 m^3		
	OUR (g·L^{-1}·h^{-1})			OUR (g·L^{-1}·h^{-1})			OUR (g·L^{-1}·h^{-1})		
	1	**4**	**7**	**1**	**4**	**7**	**1**	**4**	**7**
1	Y	Y	N	Y	Y	Y	Y	Y	Y
2	N	N	N	N	N	N	N	N	N
3	Y	Y	N	Y	Y	Y	Y	Y	Y
4	Y	Y	Y	Y	Y	Y	Y	Y	Y
5	Y	Y	N	Y	Y	Y	Y	Y	Y

The constant value of C_{OL} will influence the energies, as highlighted earlier, but there is a trade-off. Lower C_{OL} values require lower k_La values and thus lower electrical power while on the other hand giving rise to longer bioprocess times which could require more energy. Cmin simulations were performed for a number of values of C_{OL} and the results are presented in Figure 10. This shows that reducing C_{OL} has a major impact on reducing energy; there is a minimum energy but it occurs at a very low C_{OL} value around 0.05 mg·L^{-1}. It is beneficial for the simulated bioprocess to operate at this low C_{OL} value from an oxygen transfer energy perspective. However the bioprocess time was 166 hours, which is much greater than the 26.6 hours required for C_{OL} = 2 mg·L^{-1}, and this may be very disadvantageous from other perspectives such as the size of a bioreactor required to provide a specified productivity.

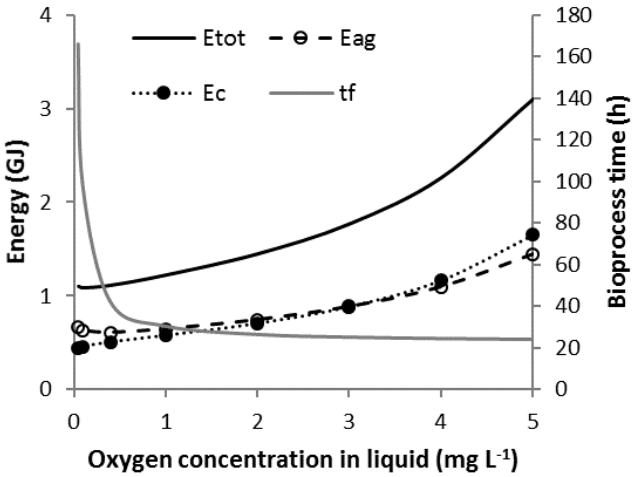

Figure 10. Scenario *Cmin*: Influence of oxygen concentration in the liquid on bioprocess time (*tf*), and agitator (*Eag*), compressor (*Ec*) and total (*Etot*) electric energies (C_{OL} = 2 mg·L^{-1}).

3.8. Scenario C1-N

The results in the previous section suggest that scenario *Cmin* may be achieved by operating at or close to the onset of flooding. This may prove impractical because it involves trying to continuously control *vvm* and *Pag* so that they are around the onset of flooding throughout the bioprocess. Furthermore, it may not be feasible from a mechanical perspective to operate the agitator at this condition throughout a bioprocess. In Scenario C1, it was shown that *Pag* has a lower limit, i.e., the critical value which is due to flooding occurring at maximum OUR. This results in a relatively high total energy requirement due to the high agitator energy requirement. As can be seen in Figure 1a, OUR is low over the first 10 hours, after which it rises progressively to its highest values, reaching these towards the end of the bioprocess. Consequently, the energy requirement can be reduced by dividing the bioprocess time up into two or more time segments with constant values of *Pag* within each segment and where different constant *Pag* values progressively increase from segment to segment up until the value in Scenario C1 in the last time segment. This is referred to as Scenario C1-N (where N is the number of time segments). Furthermore, the constant *Pag* value in each time segment could be chosen such that the onset of flooding occurs at the end of the time segment. Theoretically, an infinite number of such time segments would be the same as *Cmin* and would require the same energy. Consequently, increasing the number of time segments will reduce the energy requirement and approach *Cmin* with more and more time segments.

Figure 11a illustrates the variation in *Pag* and *vvm* for Scenario C1-5 (5 time segments) where the segments have equal time durations and the onset of flooding occurs at the end of each time segment. The values of *Pag* in each time segment represent the lowest value without having impeller flooding occur during the time segment. The non-linear increase in *Pag* from one segment to the next is due to the non-linear increase in OUR illustrated in Figure 1a. As expected, *vvm* increases within each time segment and then decreases at the transition from one segment to the next as *Pag* increases.

Simulations were performed for a number of time segments (N) to compare the energy requirements of Scenarios C1-N and C1min; the results are presented in Table 4. It can be seen that increasing the number of time segments had a major impact on reducing the total energy requirement for oxygen transfer. Dividing the bioprocess time into two time-segments had the biggest segment impact in energy reduction with a 42% energy reduction. There is a diminishing energy saving associated with each additional time segment with nearly a 66% reduction being achieved with 10 time segments. Increasing the number of segments to 100 segments gives very similar energy values to Cmin, being only 2% higher.

Table 4. Energy requirements (MJ) for the C1-N scenario with equal time segment durations (onset of flooding occurs at end of each time segment) and comparison with C1min and Cmin (C_{OL} = 2 mg·L^{-1}; % energy savings are relative to Scenario C1min).

Control Strategy	Agitator *Eag*	Compressor *Ec*	Total E_{tot}	Energy Savings (%)
C1min	4097	460	4557	-
C1-N				
C1-2	2166	464	2630	42.3
C1-5	1220	529	1749	61.6
C1-10	972	588	1560	65.7
Cmin	746	705	1415	68.1

The C1-5 scenario presented in Figure 11a used time segments with equal time durations. However, the constant *Pag* values and duration of the time segments can be varied, and this may influence the energy requirements. For example, the time segments could be divided such that a constant *Pag* step increase is applied from segment to segment and the segment time durations are varied to suit this, as illustrated in Figure 11b for C1-5. Simulations were performed for a number of time segments (N) using this time segment configuration, and the results are presented in Table 5.

The energy values are similar to those presented in Table 4 but they are noticeably higher. Thus, the time segment configuration does influence the energy values.

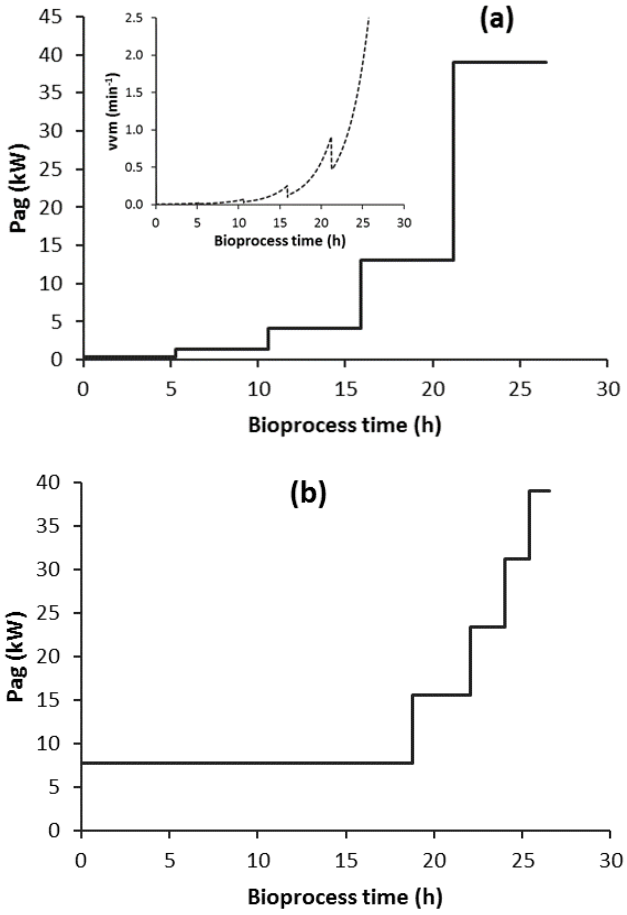

Figure 11. Scenario C1-5: (**a**) Segments with equal time durations: evolution of *Pag* and *vvm* (inset) and (**b**) constant *Pag* step increase of 7.7 kW between time segments: evolution of *Pag* (onset of flooding occurs at end of each time segment; C_{OL} = 2 mg·L^{-1}).

Table 5. Energy requirements (MJ) for C1-N scenario with constant *Pag* step increase from one time segment to the next. (C_{OL} = 2 mg·L^{-1}; onset of flooding occurs at end of each time segment).

Control Strategy	Agitator *Eag*	Compressor *Ec*	Total E_{tot}
C1-2	2279	519	2798
C1-5	1298	594	1892
C1-10	996	636	1632

To further investigate the influence of segment configuration on energy requirement, the modelling was applied to two constant *Pag* time segments (Scenario C1-2). In the second time segment the *Pag* was the critical value of *Pag*. A lower value of *Pag* was chosen in the first segment but was high enough so that the onset of flooding only occurred at the end of the time segment. The duration of the first segment at low *Pag* affects the total energy requirement, and this is illustrated in Figure 12 for a C_{OL} value of 2 mg·L^{-1}. It can be seen that there is a minimum total energy of 2.43 GJ, which occurred when the first time segment had a duration of around 19 hours and the corresponding *Pag* at the onset of flooding was 8 kW. A comparison is presented in Table 6 of this time segment configuration (C1-2min) with the two C1-2 configurations presented in Tables 4 and 5. It shows that the duration of the first-time step and size of the *Pag* step increase is in between those of the other

two configurations. It highlights that the total energy requirement is significantly lower. However, this consequential energy saving (due to segment configuration) does diminish as the number of time segments increases.

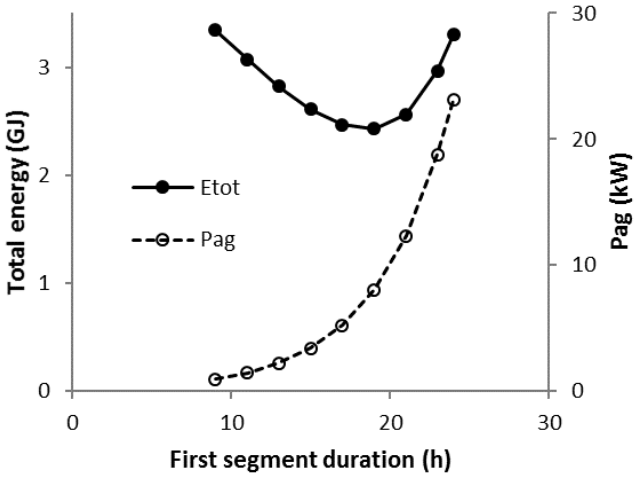

Figure 12. Scenario C1-2: Influence of the duration of the first time segment on the total electric energy requirement and *Pag* (C_{OL} = 2 mg·L^{-1}).

Table 6. Energy requirements (MJ) for time segment configurations in C1-2 (the minimum energy requirement (C1-2min), the two time segment durations are the same (Δt_{SEG} = constant), and the two *Pag* step increases are the same (ΔPag = constant)).

Control Strategy	Agitator *Eag*	Compressor *Ec*	Total E_{tot}	First Time Segment	
				Pag (kW)	Duration (h)
C1-2min	1787	642	2429	8	19
C1-2 (Δt_{SEG} = constant)	2166	460	2630	2.4	13.3
C1-2 (ΔPag = constant)	2279	519	2798	19.2	23.1

3.9. Comparison of Scenario Minimum Total Energy Requirements

Table 7 compares the minimum total energy requirements for each of the scenarios studied along with the associated agitator/compressor energies, bioprocess times and influence of C_{OL}. It also provides the percentage energy savings associated with them when compared to minimum requirement in scenario C1 (C1*min*). Table 7 shows significant variation between the minimum total energies for each scenario and thus appropriate selection of *Pag* and *vvm* can make major energy savings. *Cmin* requires only 32% of the total energy of C1*min* (C_{OL} = 2 mg·L^{-1}). The use of two appropriately chosen constant *Pag* time segments, as in C1-2min, provides a 46% energy saving over *C1min*. Furthermore, this saving represents 67% of the energy difference between C1*min* and *Cmin*. As expected, reducing C_{OL} can have a significant impact in reducing energy.

Interestingly, Kmin (where both *Pag* and *vvm* are fixed) showed a relatively low total energy requirement, which was around 30% less than C1*min* (C_{OL} = 2 mg·L^{-1}). The reason for this is somewhat complex but it is essentially because the constant *Pag* is much higher at 39 kW for *C1min* than 15 kW for *Kmin*. This is because the C_{OL} value is constrained in *Cmin* at 2 mg·L^{-1}, while it reduces to the oxygen starvation constraint value of 0.01 mg·L^{-1} in *Kmin*, as highlighted in Figure 4, where OUR increases to is highest values. The lower oxygen concentration provides a higher mass transfer driver which reduces the power requirement to provide the same OTR. Furthermore, the very low oxygen concentration did not negatively impact bioprocess time because it only occurred at the end of the bioprocess.

Table 7. Comparison of energy requirements (MJ) for the different scenarios at minimum total energy requirement within a scenario (C_{OL} = 2 mg·L^{-1}; % energy savings are relative to Scenario C1min).

Scenario	Bioprocess Time (h)	Agitator *Eag*	Compressor *Ec*	Total E_{tot}	% Energy Savings
Scenario K					
Kmin	28.8	1730	1475	3205	30
Scenario C (C_{OL} = 2 mg·L^{-1})					
C1min	26.6	4097	460	4557	-
C1-2min	26.6	1787	642	2429	46
Cmin	26.6	746	705	1451	68
(C_{OL} = 0.4 mg·L^{-1})					
C1min	42.3	3560	320	3880	15
Cmin	42.3	610	510	1120	75

4. Conclusions

Oxygen transfer in bioprocesses coupled with energy requirements is complex. Mathematical modelling can help provide a better understanding of the interactions between many variables and constraints and how these impact on energy requirements of aeration systems. Careful selection and control of *Pag* and *vvm* (and C_{OL} in Scenario C) can result in much lower total energy requirements while carrying out the same bioprocess. For example, in Scenario K the minimum total energy was 3.2 GJ at *Pag* = 15 kW, while it was 5.4 GJ at *Pag* = 45 kW. This is a large difference depending on the selection of *Pag*. Consequently, mathematical modelling of microbial kinetics, oxygen transfer and energy analysis can assist in this selection process. The modelling also highlights sensitivities of the operating conditions to oxygen concentration in the liquid, oxygen starvation, impeller flooding and phase equilibrium constraints. For Scenario K, using the k_La correlations in this study, the minimum total energy occurred at the lowest feasible *Pag* value subject to the constraints. However, this occurred at a very sensitive point, being at the intersection of the flooding and oxygen starvation constraints (Figure 2).

For Scenario C1 (where *Pag* was constant and *vvm* was varied to maintain a constant C_{OL}) the minimum total energy occurred at the lowest value of *Pag* such that the onset of flooding only occurred at maximum OUR. Overall, for Scenario C, the minimum total energy requirement was obtained when both *Pag* and *vvm* could be varied over time. For typical OUR values, it was shown that the minimum (or near minimum) total energy requirement tended to occur when operating at the flooding constraint throughout the bioprocess.

Operating at the onset of flooding may not be practical to achieve in practice. However, the study highlights that using a small number of appropriately chosen constant *Pag* time segments (Scenario C1-N) will approach the minimum total energy requirement and that this is much more practical to implement. This is possibly the most practical approach to reducing the total energy requirement and approaching the minimum seen in Scenario C.

As expected, C_{OL} has a major impact on total energy requirement, although there is a potential trade-off between oxygen mass transfer rate and microbial kinetics. In the bioprocess studied, the optimum C_{OL} value in Scenario C, which minimised total energy, was very low, but this may be problematic from other perspectives such as longer bioprocess time and the bioreactor size required to produce a given amount of product. However, it may be beneficial to operate at higher C_{OL} values of, say, 2 mg·L^{-1} when OUR and power requirements are relatively low, and then to operate at lower C_{OL} values when OUR increases towards its highest values to reduce the much higher power requirement (and overall total energy requirement) without having significant negative impacts on bioprocess time.

Overall, in the scenarios investigated, different combinations of *Pag* and *vvm* can provide the oxygen transfer required to complete the bioprocess. The selection/control of these variables can have a major impact on the oxygen transfer energy requirement and thus careful selection of these variables, in combination with C_{OL}, can help minimise the energy required, and mathematical modelling can assist in this process.

Author Contributions: J.J.F. supervised all of the work presented in the paper and wrote the paper. F.G., E.M., J.B. and A.L. contributed to the development of the mathematical models, execution of the models to generate the results and to the analysis and interpretation of the results.

Funding: This research received no external funding.

Conflicts of Interest: The authors declare no conflict of interest.

List of Symbols

A_T	cross-sectional area of bioreactor (m^2)
C_{OG}	oxygen concentration in air bubble ($mg \cdot L^{-1}$)
C_{OGI}	oxygen concentration in air entering bioreactor ($mg \cdot L^{-1}$)
C_{OGO}	oxygen concentration in air leaving bioreactor ($mg \cdot L^{-1}$)
C_{OL}	oxygen concentration in the bioprocess broth ($mg \cdot L^{-1}$)
D	impeller diameter (m)
Eag	agitator electrical energy (GJ)
Ec	compressor electrical energy (GJ)
E_{tot}	sum of agitator and compressor electrical energy (GJ)
F_G	inlet air volumetric flowrate ($m^3 \cdot h^{-1}$)
k_La	volumetric oxygen mass transfer coefficient (h^{-1})
K_O	Monod kinetic constant for oxygen ($g \cdot L^{-1}$)
K_R	Monod kinetic constant ($g \cdot L^{-1}$)
K_S	Monod kinetic constant for sugar ($g \cdot L^{-1}$)
M	Henry's Law constant
m_S	specific maintenance coefficient (h^{-1})
N	agitator rotational speed (s^{-1})
N_A	aeration number
N_{Fr}	Froude number
N_P	agitator power number (ungassed)
N_{PG}	agitator power number (gassed)
OUR	oxygen uptake rate ($g \cdot L^{-1} \cdot h^{-1}$)
OTR	oxygen transfer rate ($g \cdot L^{-1} \cdot h^{-1}$)
P	production concentration ($g \cdot L^{-1}$)
Pag	agitator mechanical power input (kW)
P_{atm}	atmospheric pressure (Pa)
P_C	compressor mechanical power input (kW)
P_i	atmospheric pressure + static head in bioreactor (Pa)
S	sugar concentration ($g \cdot L^{-1}$)
S_R	rate-limiting substrate concentration ($g \cdot L^{-1}$)
t	time (h)
t_f	bioprocess time (h)
T	bioreactor diameter (m)
V_L	bioreactor working volume (m^{-3})
vvm	volume of air per minute per unit bioreactor working volume (min^{-1})
v_s	air superficial velocity ($m \cdot h^{-1}$)
X	cell concentration ($g \cdot L^{-1}$)
Y_{XS}	yield coefficient for biomass (g dry cell weight per g sugar)
Y_{PS}	yield coefficient for product (g product per g sugar)
α, β	product production rate model constants
δ, Φ	OUR model constants
μ	specific growth rate (h^{-1})
μ_{max}	maximum specific growth rate (h^{-1})
γ	isentropic exponent of compression

References

1. Garcia-Ochoa, F.; Gomez, E. Bioreactor scale-up and oxygen transfer rate in microbial processes: An overview. *Biotechnol. Adv.* **2009**, *27*, 153–176. [CrossRef] [PubMed]
2. Bartholomew, W.H.; Karow, E.O.; Sfat, M.R. Oxygen transfer and agitation in submerged fermentations mass transfer of oxygen in submerged fermentation of *Streptomyces griseus*. *Ind. Eng. Chem.* **1950**, *42*, 1801–1809. [CrossRef]
3. Bartholomew, W.H.; Karow, E.O.; Sfat, M.R.; Wilhelm, R.H. Effect of air flow and agitation rates upon fermentation of *Penicillium chrysogenum* and *Streptomyces griseus*. *Ind. Eng. Chem.* **1950**, *42*, 1810–1815. [CrossRef]
4. Juarez, P.; Orejas, J. Oxygen transfer in a stirred reactor in laboratory scale. *Lat. Am. Appl. Res.* **2001**, *31*, 433–439.
5. Demirtas, M.U.; Kolhatkar, A.; Kilbane, J.J. Effect of aeration and agitation on growth rate of *Thermus thermophilus* in batch mode. *J. Biosci. Bioeng.* **2003**, *95*, 113–117. [CrossRef]
6. Bandaiphet, C.; Prasertsan, P. Effect of aeration and agitation rates and scale-up on oxygen transfer coefficient, kLa in exopolysaccharide production from *Enterobacter cloacae WD7*. *Carbohydr. Polym.* **2006**, *66*, 216–228. [CrossRef]
7. Huang, W.C.; Chen, S.J.; Chen, T.L. The role of dissolved oxygen and function of agitation in hyaluronic acid fermentation. *Biochem. Eng. J.* **2006**, *32*, 239–243. [CrossRef]
8. Radchenkovaa, N.; Vassilev, S.; Martinov, M.; Kuncheva, M.; Panchev, I.; Vlaev, S.; Kambourova, M. Optimization of the aeration and agitation speed of *Aeribacillus palidus418* exopolysaccharide production and the emulsifying properties of the product. *Process Biochem.* **2014**, *49*, 576–582. [CrossRef]
9. Kouda, T.; Yano, H.; Yoshinaga, F. Effect of agitator configuration on bacterial cellulose productivity in aerated and agitated culture. *J. Ferment. Bioeng.* **1997**, *83*, 371–376. [CrossRef]
10. Amanullah, A.; Tuttiett, B.; Nienow, A.W. Agitator speed and dissolved oxygen effects in xanthan fermentations. *Biotechnol. Bioeng.* **1998**, *57*, 198–210. [CrossRef]
11. Karimi, A.; Golbabaei, F.; Reza Mehrnia, M.; Neghab, M.; Kazem, M.; Nikpey, A.; Reza Pourmand, M. Oxygen mass transfer in a stirred tank bioreactor using different impeller configurations for environmental purposes. *J. Environ. Health Sci. Eng.* **2013**, *10*, 1–9. [CrossRef] [PubMed]
12. Benz, G.T. Sizing impellers for agitated aerobic fermenters. *Chem. Eng. Prog.* **2004**, *100*, 18S–20S.
13. Himmelsbach, W.; Keller, W.; Lovallo, M.; Grebe, T.; Houlton, D. Increase Productivity through better gas-liquid mixing. *Chem. Eng.* **2007**, *10*, 50–58.
14. Bakker, A.; Smith, J.M.; Meyers, K.J. How to disperse gases in liquids. *Chem. Eng.* **1994**, *12*, 98–104.
15. Hixson, A.W.; Caden, L.E., Jr. Oxygen transfer in submerged fermentation. *Ind. Eng. Chem.* **1950**, *42*, 1793–1800. [CrossRef]
16. Badino, A.C.; De Almeida, P.I.F.; Cruz, A.J.G. Agitation and aeration an automated didactic experiment. *Chem. Eng. Educ.* **2004**, *38*, 100–107.
17. Fayolle, Y.; Cockx, A.; Gillot, S.; Roustan, M.; Héduit, A. Oxygen transfer prediction in aeration tanks using CFD. *Chem. Eng. Sci.* **2007**, *62*, 7163–7171. [CrossRef]
18. Gill, N.K.; Appleton, M.; Baganz, F.; Lye, G.J. Quantification of power consumption and oxygen transfer characteristics of a stirred miniature bioreactor for predictive fermentation scale-up. *Biotechnol. Bioeng.* **2008**, *100*, 1144–1155. [CrossRef]
19. Benz, G.T. Piloting bioreactors for agitation scale-up. *Chem. Eng. Prog.* **2008**, *104*, 32–34.
20. Benz, G.T. Why conduct pilot studies for agitated gas-liquid mass transfer. *Pharm. Eng.* **2013**, *33*, 1–3.
21. Alves, S.S.; Vasconcelos, J.M.T. Optimisation of agitation and aeration in fermenters. *Bioprocess Eng.* **1996**, *14*, 119–123. [CrossRef]
22. Benz, G.T. Optimize power consumption in aerobic fermenters. *Chem. Eng. Prog.* **2003**, *99*, 32–35.
23. Benz, G.T. Cut agitator power costs. *Chem. Eng. Prog.* **2012**, *108*, 40–43.
24. Zamouche, R.; Bencheikh-Lehocine, M.; Meniai, A.H. Oxygen transfer and energy savings in a pilot-scale batch reactor for domestic wastewater treatment. *Desalination* **2007**, *206*, 414–423. [CrossRef]
25. Oliveira, R.; Simutis, R.; Feyo de Azevedo, S. Design of a stable adaptive controller for driving aerobic fermentation processes near maximum oxygen transfer capacity. *J. Process Control* **2004**, *14*, 617–626. [CrossRef]

26. Kreyenschulte, D.; Emde, F.; Regestein, L.; Büch, J. Computational minimization of the specific energy demand of large-scale aerobic fermentation processes based on small-scale data. *Chem. Eng. Sci.* **2016**, *153*, 270–283. [CrossRef]
27. van't Riet, K.; Tramper, H. *Basic Bioreactor Design*; Marcel Dekker Inc.: New York, NY, USA, 1991.
28. Znad, H.; Blazej, M.; Bales, V.; Markos, J. A kinetic model for gluconic acid production by *Aspergillus niger*. *Chem. Pap.* **2004**, *58*, 23–28.
29. Liu, J.Z.; Weng, L.; Zhang, Q.; Xu, H.; Ji, L. A mathematical model for gluconic acid fermentation by *Aspergillus Niger*. *Biochem. Eng. J.* **2003**, *14*, 137–141. [CrossRef]
30. Crueger, W.; Crueger, A. *Biotechnology: A Textbook of Industrial Microbiology*; Sinauer Associates: Sunderland, MA, USA, 1982.
31. Merchuk, J.C.; Asenjo, J.A. The Monod equation and mass transfer. *Biotech. Bioeng.* **1995**, *45*, 973–980. [CrossRef]
32. Beyenal, H.; Chen, S.N.; Lewandowski, Z. The double substrate growth kinetics of *Pseudomonas aeruginosa*. *Enzym. Microb. Technol.* **2003**, *32*, 92–98. [CrossRef]
33. Slininger, P.J.; Branstrator, L.E.; Bothast, R.J.; Okost, M.R.; Ladisch, M.R. Growth, Death, and Oxygen Uptake Kinetics of *Pichia stipitis* on Xylose. *Biotechnol. Bioeng.* **1991**, *37*, 973–980. [CrossRef] [PubMed]
34. Garcia-Ochoa, F.; Gomez, E.; Santos, V.E.; Merchuk, J.C. Oxygen uptake rate in microbial processes: An overview. *Biochem. Eng. J.* **2010**, *49*, 289–307. [CrossRef]
35. van't Riet, K. Review of measuring methods and results in non-viscous gas-liquid mass transfer in stirred vessels. *Ind. Eng. Chem. Process Des. Dev.* **1979**, *18*, 357–364. [CrossRef]